**DATING THE FORMATION OF JUPITER THROUGH W AND Mo ISOTOPE ANALYSES OF METEORITES.** T.S. Kruijer, T. Kleine, C. Burkhardt, G. Budde. University of Münster, Institut für Planetologie, Wilhelm-Klemm-Strasse 10, 48149, Münster, Germany (thomas.kruijer@wwu.de).

**Introduction:** The formation of gas-giant planets such as Jupiter and Saturn likely involved the growth of large solid cores of ~10-20 Earth masses, followed by the accumulation of gas onto these cores [1,2]. The gas-giant cores must have formed before dissipation of the solar nebula—the gaseous circumstellar disk surrounding the young Sun—which likely occurred between 1 and 10 million years (Ma) after Solar System formation. While such rapid accretion of the gas giant cores has successfully been modelled [1,2], until now it has not been possible to actually date their formation. Here we show that the growth of Jupiter can be dated using the distinct genetic heritage and formation times of meteorites.

The presence of nucleosynthetic isotope variations in bulk meteorites demonstrates that meteorites derive from genetically distinct areas within the solar accretion disk. For instance, Cr, Ti, and Mo isotope anomalies reveal a dichotomy in the genetic heritage of meteorites, distinguishing between 'non-carbonaceous' and 'carbonaceous' meteorite reservoirs [3]. This distinction may either reflect a temporal change in disk composition or the spatial separation of materials accreted inside (non-carbonaceous meteorites, NC) and outside (carbonaceous meteorites, CC) the orbit of Jupiter [3-5]. If the latter is correct, then the age of Jupiter can be determined by assessing the formation time and longevity of the non-carbonaceous and carbonaceous meteorite reservoirs. However, it is currently not known when these two reservoirs formed, and if and for how long they remained isolated from each other.

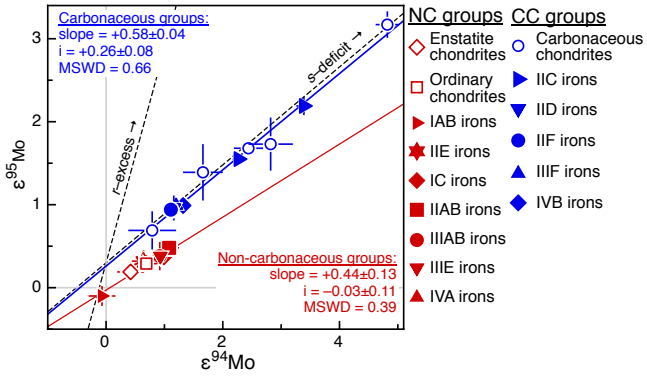


**Fig. 1:** Iron meteorites and chondrites show two distinct $\varepsilon^{95}$Mo *vs.* $\varepsilon^{94}$Mo trends, separating a carbonaceous (*blue*) from a non-carbonaceous reservoir *(red)*. Solid lines show regressions, and dashed lines, *s*- and *r*-process mixing trends [14], plotted at an ordinate $\varepsilon^{95}$Mo value of +0.3. Data from this study and from [7]. Error bars denote 95% conf. limits.

To address these issues and to ultimately assess when Jupiter formed, we obtained W and Mo isotopic data for iron meteorites by MC-ICPMS [5-7]. Iron meteorites derive from some of the earliest formed planetesimals, making them ideal samples to search for the effects of giant planet formation on the dynamics of the early solar nebula. While prior work focused on the major groups (*i.e.*, IIAB, IID, IIIAB, IVA, IVB) [6,7], we here studied a larger set of iron meteorite groups (IC, IIC, IID, IIF, IIIE, IIIF). For these samples we determined the time of core formation using the Hf-W chronometer ($t_{1/2}$ ~9 Ma), and used Mo isotope signatures to link the irons to the NC or CC meteorites.

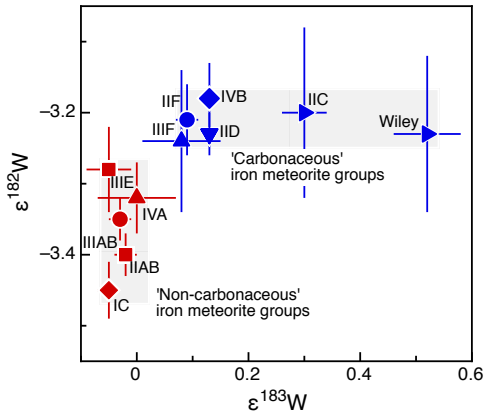


**Fig. 2:** Tungsten isotope dichotomy of iron meteorite groups. Error bars denote 95% conf. intervals on group mean values. $\varepsilon^{182}$W values were corrected for effects of nucleosynthetic heterogeneity and neutron capture [6].

**Results:** Iron meteorites show variable nucleosynthetic anomalies that predominantly reflect the heterogeneous distribution of *s*-process Mo nuclides [7]. However, in a plot of $\varepsilon^{95}$Mo *vs.* $\varepsilon^{94}$Mo (parts per $10^4$ deviations of $^{95}$Mo/$^{96}$Mo and $^{94}$Mo/$^{96}$Mo from terrestrial standard values), the iron meteorites define two distinct *s*-process mixing lines (Fig. 1). Whereas most of the newly investigated plot on an *s*-process mixing line together with carbonaceous chondrites, most of the previously investigated irons together with the IC and IIIE irons plot on a distinct *s*-process mixing line together with ordinary and enstatite chondrites, and Earth's mantle ($\varepsilon^{i}$Mo≡0) (Fig. 1). Thus, several iron meteorite groups (IIC, IID, IIF, IIIF, and IVB) belong to the carbonaceous (CC) meteorites, whereas other groups (IC, IIAB, IIIAB, IIIE, and IVA) belong to the non-carbonaceous (NC) meteorites.

A similar genetic dichotomy is seen for W isotopes, which reveal two distinct clusters of $\varepsilon^{182}$W and $\varepsilon^{183}$W

(parts per $10^4$ deviations of $^{182}W/^{184}W$ and $^{183}W/^{184}W$ from terrestrial standard values). The NC irons have $\varepsilon^{182}W$ values of *ca*. –3.4 to –3.3 and no nucleosynthetic W isotope anomalies (*i.e.*, $\varepsilon^{183}W \approx 0$), whereas the CC irons have $\varepsilon^{182}W$ values of *ca*. –3.2 and show nucleosynthetic $\varepsilon^{183}W$ excesses (Fig. 2).

**Discussion:** The higher $\varepsilon^{182}W$ of the CC irons most likely indicates a later time of core formation, at ~2.2 to ~2.8 Ma, compared to the NC irons, at ~0.5 to ~1.6 Ma after CAI formation. This difference in core formation times is most easily explained by different accretion times, and thermal modelling shows that the parent bodies of the NC irons accreted within <0.4 Ma, whereas those of the CC irons accreted at ~1 Ma after CAI formation. Collectively, the new Mo and W isotopic data indicate that accretion of CC and NC iron meteorite parent bodies not only occurred in genetically distinct nebular regions, but also at different times.

Accretion of CC iron meteorite parent bodies at ~1 Ma after CAI formation implies that by this time, the NC- and CC-reservoirs were already separated. The distinction between the NC and CC reservoirs most likely reflects the addition of *r*-process nuclide–enriched material into the solar nebula region from which the CC meteorites derive [5]. Given that all CC meteorites plot on a single *s*-process mixing line with a constant offset compared to the NC-line, they all have the same *r*-process excess relative to the NC meteorites. Consequently, this *r*-process component must have been added to and homogeneously distributed within the CC-reservoir before the first CC bodies had formed. The $^{182}W$ data for the CC irons, therefore, imply that CC reservoir formed within ~1 Ma of CAI formation, and that the separation of the NC and CC reservoirs was established by that time.

The timespan over which the NC and CC reservoirs remained separated can be inferred from the youngest accretion times of parent bodies in each reservoir. Chondrites parent bodies accreted at ~2 Ma after CAIs in the NC reservoir (ordinary chondrites) and until ~3–4 Ma in the CC reservoir (carbonaceous chondrites) [8,9]. Since in the $\varepsilon^{95}Mo$–$\varepsilon^{94}Mo$ diagram (Fig. 1), no meteorites plot between the CC- and NC-lines, the NC and CC reservoirs cannot have mixed but instead must have remained isolated from each other until parent body accretion in the NC and CC reservoirs terminated. Thus, there was no mixing between the NC and CC reservoirs until at least ~3–4 Ma after CAI formation. Of note, the accretion of ordinary chondrite parent bodies in the NC reservoir (*i.e.*, at ~2 Ma) occurred after the accretion of iron meteorite parent bodies in the CC reservoir (at ~1 Ma), meaning that the existence of the NC and the CC reservoirs cannot simply reflect a compositional change of the disk over time. Instead, the CC and NC reservoirs must have existed concurrently and remained spatially separated within the disk for several Ma.

The prolonged spatial separation of the NC and CC reservoirs could reflect a large distance between these reservoirs, but the rapid speed of grain drift in the disk renders this scenario highly unlikely [10]. Instead, the only plausible mechanism that can efficiently separate two disk reservoirs for an extended period of time is the formation of a giant planet [4,11]. The growth of Jupiter beyond >20 Earth masses ($M_E$) inhibited the inward radial drift of small particles [11], preventing any inward transport of mass. Thus, the *r*-process material that was added to the CC-reservoir did not infiltrate the coexisting yet spatially separated NC-reservoir, implying that at the time the *r*-process material was added, Jupiter already had a size of >20 $M_E$. Furthermore, since this material must have been added and homogenized before the first planetesimals formed within the CC-reservoir at ~1 Ma after CAIs, these results mandate that Jupiter reached a size of >20 $M_E$ within the first ~1 Ma after CAI formation. Once Jupiter reached a mass of 50 $M_E$, which happens via gas accretion onto its solid core, a gap opened in the disk [4,11]. This was followed by scattering of bodies from beyond Jupiter's orbit (*i.e.*, CC bodies) into the inner Solar System, either during an inward-then-outward migration of Jupiter [12], or alternatively, during runaway growth of Jupiter on a fixed orbit [13]. This scattering of CC bodies cannot have started before ~3–4 Ma after CAI formation, because carbonaceous chondrite parent bodies continued to form until at least that time [8,9]. As these chondrites plot on the CC-line in Mo isotope space (Fig. 1), they must have formed before the scattering of CC meteorites into the inner Solar System. Accordingly, these data indicate that Jupiter reached ~50 $M_E$ later than ~3–4 Ma after CAIs. This is consistent with theoretical predictions that the rapid growth of Jupiter's core to ~20 $M_E$ was followed by a more protracted stage of accretion to several tens of $M_E$ [1,2], before runaway gas accretion led to Jupiter's final mass (~318 $M_E$).

**References:** [1] Pollack J.B. et al. (1996) *Icarus* 124, 62–85. [2] Helled R. et al. (2014) in *Protostars and Planets VI*. [3] Warren P. (2016) *EPSL* 311, 93–100. [4] Morbidelli A. et al. (2016) *Icarus* 267, 368–376. [5] Budde G. et al. (2016) *EPSL* 454, 293–303. [6] Kruijer T.S. et al. (2014) *Science* 344, 1150-1154. [7] Burkhardt C. et al. (2011) *EPSL* 312, 390–400. [8] Schrader D. L. et al. (2016) *GCA*, in press. [9] Kita N.T. & Ushikubo T. (2012) *MAPS* 47, 1108–1119. [10] Birnstiel T. et al. (2013) *Astron. Astrophys.* 550, L8. [11] Lambrechts M. et al. (2014) *Astron. Astrophys*. 572, A35. [12] Walsh K.J. et al. (2011) *Nature* 475, 206–209. [13] Kretke K. A. et al. (2016) *Am. Astron. Soc. DPS Meeting* #48. [14] Nicolussi G. K. et al. (1998) *GCA* 62, 1093–1104.